# Erbium-doped CW and $Q$-switched fiber ring laser with fiber grating Michelson interferometer

**Anting Wang (王安廷), Hai Ming (明 海), Jianping Xie (谢建平), Lixin Xu (许立新), Wencai Huang (黄文财), Liang Lü (吕 亮), Xiyao Chen (陈曦曜), Feng Li (李 锋), Yunxia Wu (吴云霞), and Meishu Xing (邢美术)**

*Department of Physics, University of Science & Technology of China, Hefei 230026*

Received July 13, 2002

The band-pass characteristic of fiber grating Michelson interferometer is analyzed, which acts as both band-pass filter and $Q$-switch. An erbium-doped fiber ring laser based on fiber grating Michelson interferometer is implemented for producing single longitudinal mode CW operation with 5 MHz spectral linewidth and up to 6 mW output power. In $Q$-switched operation, stable fiber laser output pulses with repetition rate of 800 Hz, pulse width of 0.6 $\mu$s, average power of 1.8 mW and peak power of 3.4 W are demonstrated. The peak power and average power of the $Q$-switched pulses are varied with the repetition rate.

*OCIS codes:* 140.3540, 140.3570, 140.3500, 140.3510.

Recently, fiber grating technology, fiber lasers and fiber amplification have attracted considerable interest because of their applications in optical communication. $Q$-switched erbium-doped fiber lasers are useful for applications such as sensing and laser range finding. Continuous output, $Q$-switched and mode-locked fiber lasers have been reported. In $Q$-switching technology, all-fiber $Q$-switched lasers with wavelength tunable, fiber grating $Q$-switching lasers and self-$Q$-switched lasers have been reported[1−3]. Fiber ring laser can prevent spatial-hole burning (SHB) and can get narrow linewidth and single longitudinal mode (SLM) laser with band filter[4−6]. In this paper, we present a novel erbium-doped CW and $Q$-switched fiber ring laser with narrow linewidth, in which a Michelson interferometer acts as band-pass filter and $Q$-switch.

The structure of fiber grating Michelson interferometer is shown in Fig. 1. It is composed of a 3 dB fiber coupler and two same fiber gratings. Its transmission matrix is

$$T_2 = \frac{1}{4}[\sigma_1^2|r_1|^2 + \sigma_2^2|r_2|^2 + 2\sigma_1\sigma_2|r_1||r_2|\cos\delta]\sin^2(2\kappa L_c), \quad (1)$$

where $r_j (j = 1, 2)$ is the amplitude reflection coefficient of the grating, $\delta$ is the phase difference between the reflections from the two gratings at port 2, $\sigma_1$ and $\sigma_2$ are the additional factors that are related with the polarization and loss of the two arms, $\kappa$ is the coupling constant and $L_c$ is the coupling length of the fiber coupler.

The reflection coefficient of the grating is given as

$$r_j = \frac{-\kappa_{ac}\sinh(\alpha L)}{\eta\sinh(\alpha L) - i\alpha\cosh(\alpha L)} = |r_j|\exp[i\varphi_j(\lambda)] \quad (j = 1, 2), \quad (2)$$

where $\kappa_{ac}$ is the ac coupling constant and $\eta$ is the dc coupling constant of fiber grating, $L$ is the length of grating, and

$$\alpha = \sqrt{|\kappa_{ac}|^2 - \eta^2}. \quad (3)$$

The phase difference between the reflections from the two gratings is given as

$$\delta = 2\left[\frac{2\pi n_{eff}}{\lambda}\Delta l + \frac{\varphi_2(\lambda) - \varphi_1(\lambda)}{2}\right] = 2\left[\frac{2\pi n_{eff}}{\lambda}\Delta l + \frac{\Delta\varphi_{21}(\lambda)}{2}\right], \quad (4)$$

where $\Delta l$ is the physical path length difference between the two arms of Michelson interferometer, $n_{eff}$ is the effective refractive index of fiber, $\lambda$ is the Bragg wavelength of the fiber grating, $\varphi_j(\lambda)$ described by Eq. (2) is the phase of grating, $\Delta\varphi_{21}(\lambda) = \varphi_2(\lambda) - \varphi_1(\lambda)$ is the differential phase of the two gratings.

For 3 dB fiber coupler, $\kappa L_c = \pi/4$; ignoring loss and polarization effects and assuming Bragg wavelengths and center reflectivities are exactly the same for the two gratings, Eq. (1) is simplified to

$$T_2 = \frac{1}{2}\frac{\kappa_{ac}^2\sinh^2(\alpha L)}{\eta^2\sinh^2(\alpha L) + \alpha^2\cosh^2(\alpha L)} \times \left[1 + \cos\left(\frac{4\pi n_{eff}}{\lambda}\Delta l\right)\right]. \quad (5)$$

The band-pass characteristic of fiber grating Michelson interferometer is shown in Fig. 2. Figure 2(a) is band-pass characteristic when interference peak wavelength and Bragg wavelength are the same, while Fig. 2(b) is the band-pass characteristic when the interference phase changes by $\pi$ (i.e. the path length difference between the two arms changes by 0.24699 $\mu$m). The $Q$-switch property is better for smaller path length difference. When fiber grating Michelson interferometer acts as $Q$-switch, the tuning resolution

$$\frac{d\lambda}{d(\Delta l)} = \frac{\lambda}{\Delta l}. \quad (6)$$

From the above, one can see tuning resolution is inversely proportional to $\Delta l$, i.e. the smaller the $\Delta l$, the higher the tuning resolution.

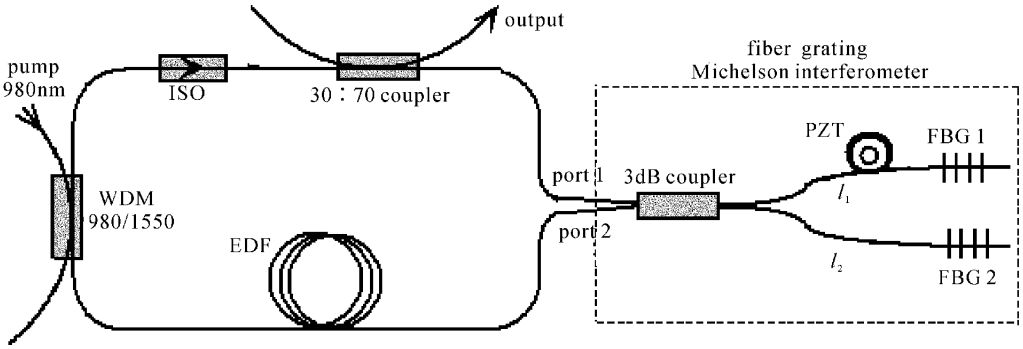


Fig. 1. Configuration of single-frequency $Q$-switched Er-doped fiber ring laser.

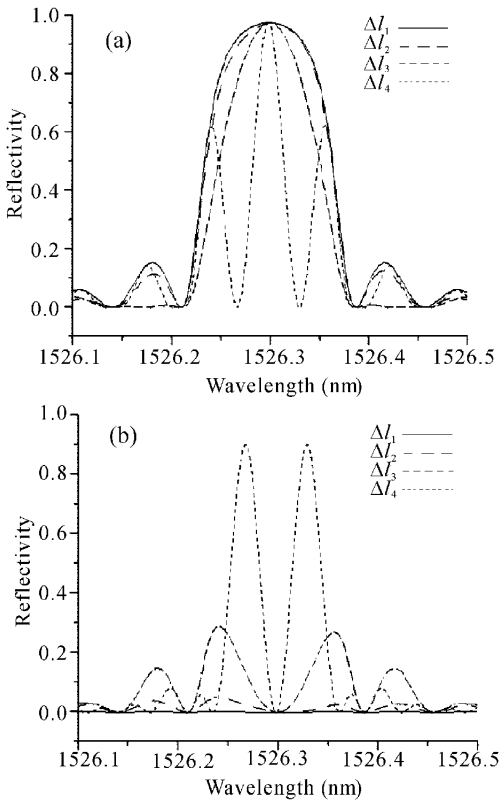


Fig. 2. The band-pass characteristic of fiber grating Michelson interferometer. (a) Band-pass characteristic for the same peak wavelength and Bragg wavelength: $\Delta l_1$=0.19957 nm; $\Delta l_1$=1.00082 nm; $\Delta l_3$=2.99997 nm; $\Delta l_4$=11.99987 nm. (b) Band-pass characteristic for phase change of $\pi$ (change of $\Delta l$ is about 0.24699 $\mu$m).

Figure 1 shows a schematic diagram of the experimental setup employed to produce the single-frequency $Q$-switched fiber ring laser. A 980/1550 nm wavelength division multiplexing (WDM) coupler is used to provide 980 nm pump power from a semiconductor laser (center wavelength at 976 nm, linewidth is 0.8 nm and maximum output power 110 mW). The 4-meter erbium-doped fiber has a doping concentration of 280 ppm, core diameter of 3 $\mu$m and cutoff wavelength of 920 nm. An optical isolator (ISO) is used to make laser propagation in a clockwise direction in a traveling-wave pattern. A 30:70 coupler is used as the output coupler of the laser. At every arm's end, the two gratings are the same and have a reflectivity of 99%, bandwidth of 0.15 nm, and center wavelength of 1526.30 nm. The path length difference between the two arms of the Michelson interferometer is 0.19 mm, and one of the arms is winded firmly on a piezoelectric transducer (PZT), which can act as both band-pass filter and $Q$-switch.

Under CW conditions in the absence of the PZT, the laser spectrum is observed with an ANDO AQ6317B optical spectrum analyzer with a 0.02 nm resolution, as shown in Fig. 3. The mode suppressed ratio (MSR) is over 41 dB at 1526.30 nm. The insert in Fig. 3 shows the relation between the fiber laser output power and the pump power. The threshold pump power is 20 mW, the slope efficiency is 8.25% at 1526.30 nm, and the output power is greater than 6 mW. Using spherical Fabry-Perot interferometer (MODEL 240 spectrum analyzer) having a free spectral range (FSR) of 7.5 GHz and a resolution of 5 MHz, the corresponding scan display of the output spectrum is shown in Fig. 4. Figure 4(a) shows the output spectrum, confirming the SLM nature of the laser oscillation. Figure 4(b) is an expanded view of one of the resonances in Fig. 4(a), and the spectral linewidth is 5 MHz. Because of the limitation of 5 MHz resolution of the spectrum analyzer used, the potential linewidth of the fiber laser less than 5 MHz can be expected.

In the $Q$-switched operation, a sinusoid voltage signal of 14 V in amplitude and 800 Hz in frequency is applied to the PZT to get high power $Q$-switched pulse output with the same pulse frequency as the modulation frequency, pulse width of 0.6 $\mu$s, peak power of 3.4 W and average power of 1.8 mW. Figure 5 shows the output pulses measured by an InGaAs pin photodetector

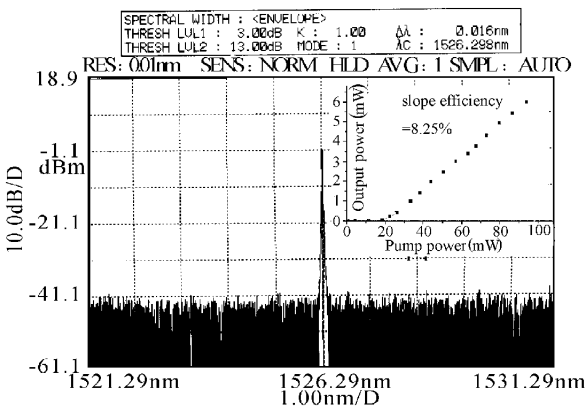


Fig. 3. The laser spectrum of the CW erbium-doped fiber ring laser. The insert is output laser power versus pump power.

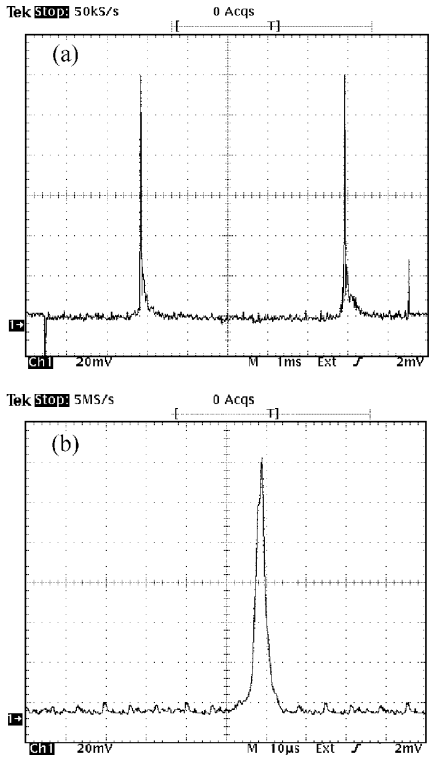


Fig. 4. The output spectrum measured by MODEL 240 spectrum analyzer (reslution is 5 MHz). (a) The PSR is about 7.5 GHz. (b) The expanded view of (a), spectral linewidth of the laser being 5 MHz.

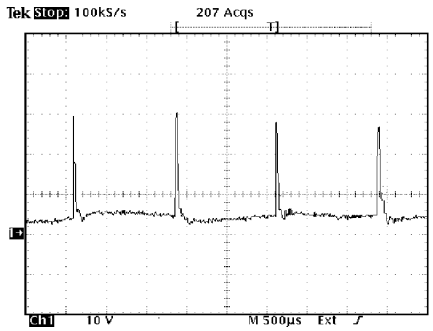


Fig. 5. A typical output pulses train for the pulse repetition rate of 800 Hz.

and a 400 MHz digital oscilloscope. The average power and the peak power at different repetition rates are measured and the results are shown in Fig. 6. The decrease in peak power with increasing repetition rate is due to the finite recovery time of the population inversion in the pumped erbium-doped fiber when the fiber laser is in the low-$Q$ state.

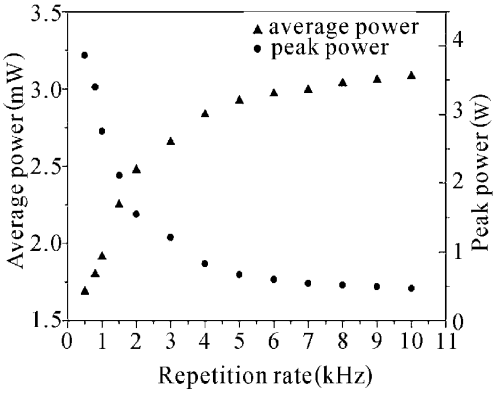


Fig. 6. Average power (triangles) and peak power (dots) versus repetition rate in $Q$-switched regime of operation.

The band-pass characteristics, as well as $Q$-switch property of fiber grating Michelson interferometer are ana-lyzed. The Michelson interferometer offers wavelength selecting as well as $Q$-switching functions. A stable CW SLM Er-doped fiber ring laser is fabricated, which is basically structured on a fiber grating Michelson interferometer. The laser can provide up to 6 mW continuous output power at 1526.30 nm. The SLM is securely attained with a narrow linewidth of 5 MHz which is limited by the resolution of scanning spherical Fabry-Perot interferometer. A stable $Q$-switched fiber ring laser at 1526.30 nm with a peak power of 3.4 W, average power of 1.8 mW, repetition rate of 800 Hz and pulse width of 0.6 $\mu$s, is demonstrated. The peak power and average power of the $Q$-switched pulses are varied with the repetition rate.

This work was supported by the Natural Science Foundation of Anhui Province, China under Grant No. 01042402. A. Wang's e-mail address is atwang@mail.ustc.edu.cn.

## References

1. L. X. Xu, H. Ming, W. An, X. S. Zhang, A. T. Wang, W. Li, L. Wang, J. P. Xie, Y. X. Wu, Z. Q. Lin, L. R. Chen, B. Chen, S. H. Chen, H. B. Yin, and Y. X. Liu, Chin. J. Lasers B **9,** 385 (2000).
2. W. C. Du, H. Y. Tan, and S. H. Liu, Acta Optica Sinica (in Chinese) **17,** 1077 (1997).
3. S. V. Chernikov, Y. Zhu, J. R. Taylor, and V. D. Gapontsev, Opt. Lett. **22,** 298 (1997).
4. N. Park, J. W. Dawson, K. J. Vahala, and C. Miller, Appl. Phys. Lett. **59,** 2369 (1991).
5. S. Yamashita and K. Hsu, Opt. Lett. **23,** 1200 (1998).
6. J. L. Zhang, C. Y. Yue, G. W. Schinn, W. R. L. Clements, and J. W. Y. Lit, J. Lightwave Technol. **14,** 104 (1996).